



X International Conference on Structural Dynamics, EURODYN 2017

# Optimization of a Pseudoelastic Absorber for Vibration Mitigation

Vinicius Piccirillo<sup>a,\*</sup>, Davide Bernardini<sup>b</sup>, Giuseppe Rega<sup>b</sup>

<sup>a</sup>UTFPR, Monteiro Lobato Avenue, Ponta Grossa, 84040-050, Brazil

<sup>b</sup>Dipartimento di Ingegneria Strutturale e Geotecnica, Sapienza Università di Roma

---

## Abstract

Dynamic vibration absorbers (DVAs) have received special attention in recent years due to their capability to reduce structural vibrations of a primary structure. In this work, a DVA of the Tuned Mass Damper type based on a Shape Memory Alloy (SMA) element with pseudoelastic behavior is considered. Owing to their rich thermomechanical response, SMAs can exhibit hysteresis loops with rather different features in terms of overall energy dissipation and of pseudoelastic stiffness. As a first step towards the comprehensive evaluation of the performances of such a device, the optimization of a TMD based on SMA devices with different features is studied. Numerical simulations show that the size and the shape of the pseudoelastic loops can influence in a significant way the performances of the DVA.

© 2017 The Authors. Published by Elsevier Ltd.

Peer-review under responsibility of the organizing committee of EURODYN 2017.

*Keywords:* Shape memory alloy; pseudoelasticity; dynamical vibration absorber; optimization

---

## 1. Introduction

Among the various strategies for structural vibrations control, Tuned Mass Dampers (TMDs), also known as Dynamic Vibration Absorbers (DVAs), received considerable attention in the recent years.

The typical setting for DVAs is the so-called linear TMD that consists of a mass connected by an elastic spring and a viscous damper to the main structure to be protected (Fig. 1). Vibration damping is then realized through the energy transfer from the primary to the secondary structure that takes places in a suitable range of frequencies.

---

\* Corresponding author. Tel.: +55-4232357056.

E-mail address: [piccirillo@utfpr.edu.br](mailto:piccirillo@utfpr.edu.br)

The performances of a TMD are usually evaluated by means of two degrees of freedom systems, so that the damping of the device is crucial to avoid resonances and to promote the oscillations of the secondary mass at the expense of those of the main structure.

One of the most important aspects related to the design of this type of devices is the tuning of the various parameters that define a specific configuration, such as: mass, natural frequency and damping ratios between the primary and secondary systems. To this end, various strategies can be used depending on the features of the device and the main structure and, in fact, a large number of studies that propose different methods for the optimization of the DVAs parameters is available in the literature.

The classical approach for the tuning of a linear TMD under harmonic forcing is the equal-peak method originally presented in [1] for an undamped primary structure. In this classical setting, the optimal damping and frequency parameters of the DVA can be expressed as a function of the mass ratio in such a way to get a frequency-response curve of the primary structure with two peaks of equal intensity. This approach is closely related to the  $H_\infty$  optimization which minimizes the oscillation amplitude of the main structure [2]. Another tuning strategy is the so called  $H_2$  optimization which aims to minimize the vibration energy transmitted by the forcing excitation to the main structure by optimizing the squared area under its frequency-response curve. Whereas in the case of an undamped main structure the solutions of these optimization problems are well-known and available in closed form, the corresponding solutions for a TMD attached to a damped structure are less straightforward and the problem is usually tackled either by approximate analytical solutions [2,3,5] or by numerical simulations [4,6].

Since the performances of TMDs are influenced in a crucial way by the damping of the secondary system, it is natural to ask if devices with energy dissipation features different from the basic viscous damping can be useful in the development of DVAs. This question leads to the study of nonlinear TMDs based on masses connected to the main structure by a restoring force with hysteretic behavior [7].

Among the many options available to realize hysteretic TMDs, Shape Memory Alloys (SMAs) offer a promising alternative. SMAs are a group of metallic materials that exhibit special functional properties (shape memory effect, pseudoelasticity, pseudoplasticity) as a consequence of the occurrence of solid phase transformations at the microscopic scale. When SMAs are used to obtain pseudoelastic behavior, the material exhibits hysteresis with high damping without residual displacements [8].

In this paper, the response of a hysteretic TMD based on a pseudoelastic SMA device is investigated. Due to the thermomechanical coupling typical of the phase transformations that occur in SMA, significant temperature variations arise during mechanical loading and a careful constitutive modeling is necessary. To this end a thermomechanical model is utilized to describe the restoring force of the device [8]. Moreover, since the SMA model can exhibit hysteresis loops with different features, various combinations of the underlying parameters are considered.

## 2. The pseudoelastic TMD

A TMD composed of a main mass  $m_1$  connected to a secondary mass  $m_2$  via a SMA device with pseudoelastic behavior is considered (Fig. 1). The thermomechanical model used to represent the pseudoelastic restoring force is described in [8] and has been successfully applied to the study of nonlinear dynamics of SMA oscillators [9,10]. The equations of motion of the two-d.o.f. system subject to an harmonic forcing on the main structure are:

$$\begin{aligned} m_1 \ddot{x}_1 - c_2 (\dot{x}_2 - \dot{x}_1) + c_1 \dot{x}_1 + k_1 x_1 - f_{SMD} &= F_0 \cos(\omega t) \\ m_2 \ddot{x}_2 + c_2 (\dot{x}_2 - \dot{x}_1) + f_{SMD} &= 0 \end{aligned} \quad (1)$$

where:  $f_{SMD} = K[(x_2 - x_1) - \text{sgn}(x_2 - x_1)\delta\xi^e]$ ,  $K$  is the stiffness of the SMA device which is assumed to be constant and equal to the fully austenitic state,  $\delta$  is the maximum transformation displacement and  $\xi$  is the volume fraction of Martensite. For the sake of conciseness, in this work, the attention is focused on the isothermal response whereas the analysis of the influence of the full thermomechanical coupling will be presented elsewhere. To describe SMA

behavior, equations of motion (1) need to be complemented by a transformation kinetics that governs the evolution of the phase fraction [8]. While doing this, it turns out to be useful to rewrite (1) in dimensionless form so as to give:

$$\begin{aligned} \ddot{u}_1 + 2\zeta_1\dot{u}_1 - 2\zeta_2\mu\rho_{SMA}(\dot{u}_2 - \dot{u}_1) + u_1 - \rho_{SMA}^2\mu[(u_2 - u_1) - \text{sgn}(u_2 - u_1)\lambda\xi] &= A\cos(\Omega\tau) \\ \ddot{u}_2 + 2\zeta_2\rho_{SMA}(\dot{u}_2 - \dot{u}_1) + \rho_{SMA}^2[(u_2 - u_1) - \text{sgn}(u_2 - u_1)\lambda\xi] &= 0 \\ \dot{\xi} &= Z[\text{sgn}(u_2 - u_1)(\dot{u}_2 - \dot{u}_1) - JQ] \end{aligned} \tag{2}$$

The non-dimensional quantities are:

$$u_1 = \frac{x_1}{x_{MS}}, u_2 = \frac{x_2}{x_{MS}}, \zeta_2 = \frac{c_2}{2m_2\omega_2}, \zeta_1 = \frac{c_1}{2m_1\omega_1}, \omega_1 = \sqrt{\frac{k_1}{m_1}}, \omega_2 = \sqrt{\frac{K}{m_2}}, \tau = \omega_1 t, A = \frac{F_0}{m_1\omega_2^2 x_{MS}}, \Omega = \frac{\omega}{\omega_1}$$

where  $x_{MS}$  is the displacement at the onset of the upper pseudoelastic plateau and  $\omega_1$  and  $\omega_2$  are the natural frequencies of the primary system and of the absorber.

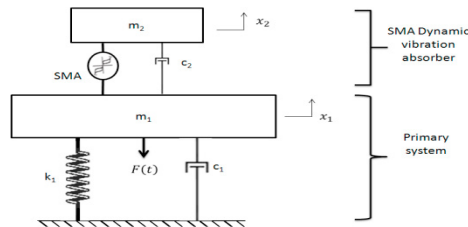


Figure 1: Primary system with SMA dynamical vibration absorber

The features of the SMA behavior are implemented via the function  $Z$  in the third one of (2). The explicit expression of  $Z$  is discussed in [8] where the precise meaning of all the parameters involved is also explained. For the purpose of this analysis it suffices to say that  $Z$  depends, among the others, on two basic parameters  $q_1, q_2$  that determine the basic shape of the pseudoelastic loops observed in isothermal conditions. As discussed in [8],  $q_1$  and  $q_2$  influence, respectively, the slopes of the upper and the lower plateaus and physically meaningful ranges can be identified with  $q_1 \in [0.7, 1.0]$  and  $q_2 \in [1.0, 1.3]$ . Besides the above two SMA parameters, there are two basic quantities that influence the behavior of the TMD, namely the mass and natural frequency ratios between the device and the main structure:  $\mu = \frac{m_2}{m_1}, \rho_{SMA}^2 = \frac{\omega_2^2}{\omega_1^2}$ .

In order to illustrate the main features of the dynamic response of the TMD, Figure 2 shows a typical Frequency-Response Curve (FRC). The curve is obtained for a mass ratio  $\mu = 0.05$  and a low value for the damping of both the absorber and the primary system, namely  $\zeta_1 = 0.03$  and  $\zeta_2 = 0.03$ . This choice is made in order to highlight the influence of the sole SMA device dissipation. It is clear that the performances of an actual TMD can be significantly increased by additional viscous damping, but this aspect is not discussed here.

The stiffness of the TMD is determined by the frequency ratio  $\rho_{linear} = 0.9527$  which is obtained by using the approximate analytic formula

$$\rho_{linear} = \frac{\omega_2}{\omega_1} = \sqrt{\frac{1 - 4\zeta_1^2 - \mu(2\zeta_1^2 - 1)}{(1 + \mu)^3}} \tag{3}$$

proposed in [5], via fixed-point theory, as optimal tuning of a linear TMD attached to a damped primary system.

Figure 2 shows the FRC of the main structure corresponding to a small forcing amplitude  $A = 0.05$  and the force-displacement curves of the SMA absorber at some specific points. It turns out that the use of the frequency ratio  $\rho$  given by (3) yields a FRC with peaks that do not have the same level, hence the tuning of this type of TMD differs significantly from the one of linear TMDs.

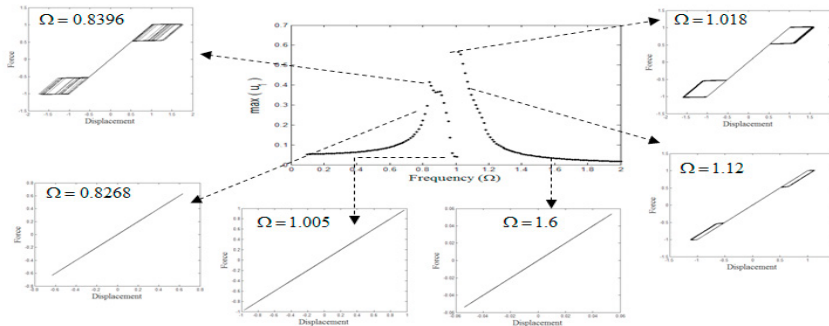


Figure 2: Frequency Response Curve of the main structure for excitation amplitude  $A = 0.05$  and  $q_1 = 0.98$  and  $q_2 = 1.2$

Since the overall linear damping level is low, the FRC shows the typical shape with two sharp peaks and a valley close to zero in the perfect tuning conditions. The two peaks in the main structure response correspond to oscillations of the SMA absorbers where significant phase transformations take place.

An additional phenomenon which is not discussed here in detail but should be remarked is the fact that, for higher amplitude levels, the FRC of the absorber tends to exhibit jump phenomena of the type documented for example in [8] as a consequence of the occurrence of solutions with complete phase transformations. When the SMA undergoes such jumps, a similar behavior can be observed also in the primary structure. This phenomenon can be avoided by designing some additional linear damping to be added to the main structure or to the absorber.

### 3. TMD optimization strategy

The previous example showed that the tuning criteria typically used for linear TMD do not work in this case so that alternative strategies need to be used. Generally speaking, TMD optimization aims to minimize the oscillations of the primary system in the largest possible range of excitation frequency.

Various aspects of the FRC can be optimized. The  $H_\infty$  optimization attempts to minimize the level of the peaks of the curve which correspond to the maximum oscillation amplitude in the main structure. This procedure typically achieves also the equal-peaks criterion. On the other hand,  $H_2$  optimization focuses on the area under the FRC so as to minimize the energy transferred to the structure. In this case one can perhaps accept a slightly higher level of the peaks but with a flatter curve that ensures a larger frequency tuning range.

In the following, the  $H_\infty$  strategy is applied to the system by solving numerically the following optimization problem. If the FRC of the main structure is denoted as a function  $G$  of the dimensionless frequency  $\Omega$ , the frequency ratio  $\rho$ , and the model parameters  $q_1$  and  $q_2$ , namely,  $G(\rho, q_1, q_2, \Omega)$ , the aim here is minimizing the maximum of  $G(\rho, q_1, q_2, \Omega)$ ,  $\forall \Omega$ . The optimization problem proposed in this paper as optimal tuning strategy can be formulated as follows:

$$\min_{\rho, q_1, q_2} H_\infty := \min_{\rho, q_1, q_2} \left( \max_{i=1}^N \left( |G(\rho, q_1, q_2, \Omega_i)| \right) \right) \tag{4}$$

As it will be shown in the next Section, this procedure turns out to be very efficient to optimize the SMA hysteretic TMD.

#### 4. Basic aspects of the TMD performances

It is well known that SMAs can exhibit hysteresis loops with rather different features, depending on the type of alloys used, the metallurgical treatments, as well as on the specific arrangement of the material chosen to realize the device that actually produces the restoring force [8].

More specifically, it is possible to realize SMA devices with higher or lower hysteresis as well as devices with different post-elastic stiffness of the plateaus. It is evident that both the amount of hysteresis and the stiffness of the pseudoelastic plateaus will influence in a significant way the performances of the TMD. These two aspects can be easily controlled in the constitutive model by the values of the two parameters  $q_1$  and  $q_2$ .

To this end, the optimization and the response of the TMD is now analyzed under two conditions that can be considered as limit cases that, in some sense, bound all the other possibilities. Case 1 is characterized by  $q_1 = 0.98$  and  $q_2 = 1.02$  that correspond to a device with hysteresis loop which can be defined as “flat and thin” (Fig. 3a). On the other hand, Case 2 is characterized by  $q_1 = 0.7$  and  $q_2 = 1.2$  that yield a “steeper and thicker” loop (Fig. 3b).

The 3D plots of the FRC as a function of the natural frequency ratio  $\rho$  are shown in Figures 4(a) and 5(a) for the two types of devices. These three dimensional surface plots provide an overview of the dynamic behavior of the system. The optimal value of  $\rho_{SMA}$  is then determined, according to the procedure described in Section 3, by minimizing the  $H_\infty$ - norm of the FRC. Figures 4(b) and 5(b) show the  $H_\infty$ - norm curves plotted as function of  $\rho_{SMA}^{-1}$ . Both curves present a global minimum corresponding to the optimal solution. In Fig. 4(b) the minimum occurs for  $\rho_{SMA} = 0.8$ , while in Fig. 5(b) the minimum occurs for  $\rho_{SMA} = 0.9579$ . The black lines in the Figs. 4(a) and 5(a) highlight the optimal FRCs which are better shown in Figs. 4(c) and 5(c). Figure 6 finally shows the comparison between the two cases. This points out that the optimization procedure gives rise to a curve with equal peaks as the one which minimizes the maximum level of oscillations in the main structure. As expected, Case 2, being characterized by higher damping, gives better performances. Due to the small damping generated by the SMA device in Case 1, an additional small peak emerges between the two main ones in the relevant FRC.

#### 5. Conclusions

The basic aspects of the optimization and of the performances of DVAs realized with SMA elements have been investigated in two limit cases of hysteresis loops with different dissipative properties. The optimization based on the  $H_\infty$ - norm provides an effective tool to determine the optimal value of the natural frequency of the device in both cases. Good performances in terms of vibration attenuation are obtained, showing that SMA can be considered as a promising solution for the realization of hysteretic TMDs. Of course, the actual level of performance increases with the width of the pseudoelastic loops and could be further improved by the addition of further viscous damping. A comprehensive analysis of the performances of the SMA-based TMD, including a comparison with conventional linear ones under different excitation amplitudes is under development also taking into account the full thermomechanical coupling and will be reported elsewhere.

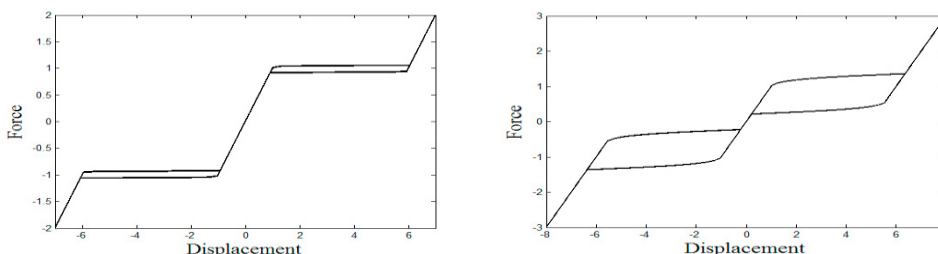


Figure 3: Force-displacement curves for the two SMA devices considered: (a) Case 1, (b) Case 2.

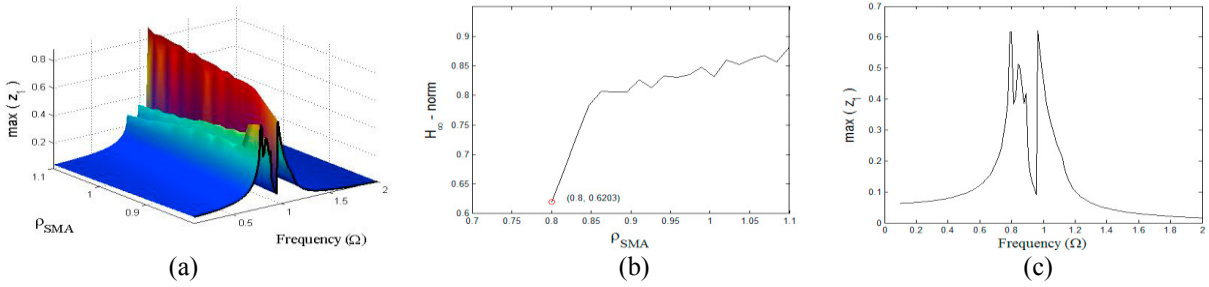


Figure 4: (a) 3D FRC, (b)  $H_\infty$  - norm vs.  $\rho_{SMA}$  and (c) FRC for optimal value  $\rho_{SMA}$

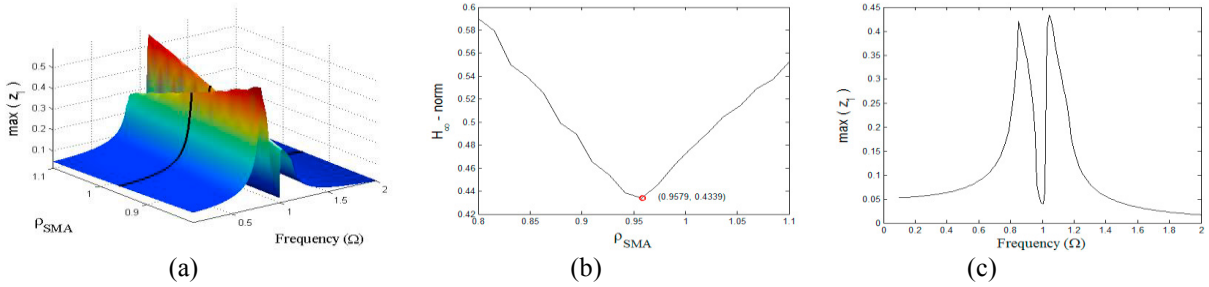


Figure 5: (a) 3D FRC, (b)  $H_\infty$  - norm vs.  $\rho_{SMA}$  and (c) FRC for optimal value of  $\rho_{SMA}$

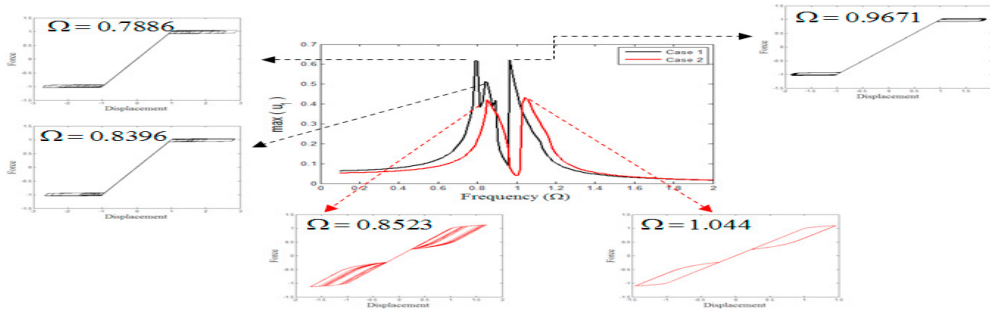


Figure 6: Comparison of the Frequency Response Curve for Case 1 and Case 2

References

- [1] J. Den Hartog, Mechanical Vibrations, 4th ed., McGraw-Hill, New York., 1956.
- [2] T. Asami, O. Nishihara, Closed-form exact solution to  $h_\infty$  optimization of dynamic vibration absorbers (application to different transfer functions and damping systems). *J. Vib. Acoust.* 125 (2003) 398–405.
- [3] T. Asami, O. Nishihara, A. Baz, Analytical solutions to  $H_\infty$  and  $H_2$  optimization of dynamic vibration absorbers attached to damped linear systems, *ASME J. Vib. Acoust.* 124 (2002) 284–295.
- [4] H.C.Tsai,G. .C Lin, Explicit formulae for optimum absorber parameters for force-excited and viscously damped systems, *J. Sound Vib.* 176 (1994) 585–596.
- [5] A. Ghosh, B. Basu, A closed-form optimal tuning criterion for TMD in damped structures, *Struct. Control Health Monit.* 14 (2007) 681–692.
- [6] S. Randall, D. Halsted, D. Taylor, Optimum vibration absorbers for linear damped systems, *ASME J. Mech. Des.* 103 (1981) 908–913.
- [7] N. Carpineto, W. Lacarbonara, F. Vestroni, Hysteretic tuned mass dampers for structural vibration mitigation, *J. Sound Vib.* 333 (2014) 1302–1318.
- [8] D. Bernardini, G. Rega, Chaos robustness and strength in thermomechanical shape memory oscillators Part I: A predictive theoretical framework for the pseudoelastic behavior, *Int. J. Bifurcation and Chaos.* 21 (2011) 2769–2782.
- [9] V. Piccirillo, J.M Balthazar, A.M Tusset, D. Bernardini, G. Rega, Non-linear dynamics of a thermomechanical pseudoelastic oscillator excited by non-ideal energy sources, *Int. J. Non-Lin. Mech.* 77 (2015) 12-27.
- [10] D. Bernardini, G. Rega, Chaos robustness and strength in thermomechanical shape memory oscillators Part II: Numerical and theoretical evaluation, *Int. J. Bifurcation and Chaos.* 21 (2011) 2783–2800.